Reference transcriptome data in silkworm *Bombyx mori*

Kakeru Yokoi[1,2,*,**], Takuya Tsubota[3,*], Jianqiang Sun[2], Akiya Jouraku[1], Hideki Sezutsu[3], Hidemasa Bono[4]

1 Insect Genome Research and Engineering Unit, Division of Applied Genetics, Institute of Agrobiological Sciences (NIAS), National Agriculture and Food Research Organization (NARO), 1-2 Owashi, Tsukuba, Ibaraki 305-8634, Japan
2 Research Center for Agricultural Information Technology (RCAIT), National Agriculture and Food Research Organization (NARO), Kintetsu Kasumigaseki Building Kasumigaseki 3-5-1 Chiyoda-ku, Tokyo 100-0013, Japan
3 Transgenic Silkworm Research Unit, Division of Biotechnology, Institute of Agrobiological Sciences (NIAS), National Agriculture and Food Research Organization (NARO), 1-2 Owashi, Tsukuba, Ibaraki 305-8634, Japan
4 Database Center for Life Science (DBCLS), Joint Support-Center for Data Science Research, Research Organization of Information and Systems, 1111 Yata, Mishima, Shizuoka 411-8540, Japan
*These authors equally contributed to this work.
**Corresponding author: Kakeru Yokoi

Email adresses
Kakeru Yokoi: yokoi123@affrc.go.jp
Takuya Tsubota: tsubota@affrc.go.jp
Sun Jianqiang: j.sun@affrc.go.jp
Akiya Jouraku: joraku@affrc.go.jp
Hideki Sedutsu: hsezutsu@affrc.go.jp
Hidemasa Bono: bono@dbcls.rois.ac.jp

Abstract

The silkworm *Bombyx mori* has long been used in the silk industry and utilized in studies of physiology, genetics, molecular biology, and pathology. We recently reported high quality reference genome data for *B. mori.* In the present study, we constructed a

reference transcriptome data set using the reference genome data and RNA-seq data of 10 tissues from P50T strain larvae. Reference transcriptome data contained 51,926 transcripts, with 39,619 having one or more coding sequence region. The abundance of each transcript in the 10 tissues as well as 5 tissues from other strain larvae was estimated, and hierarchical clustering was performed. The results obtained showed that data on abundance were highly reproducible and there here is a little difference of transcriptome abundance between the two strain larvae. New isoforms of silk-related genes were searched for in the reference transcriptomes, and the longest isoform of *sericin-1* possessing a long exon was identified. We also extracted transcripts that were strongly expressed in one or more parts of the silk glands. An enrichment analysis performed using the functional annotation data of the transcripts provided novel insights into the functions of the silk gland parts. Therefore, the reference transcriptome data set obtained has extended *B. mori* genomic and transcriptomic insights and may contribute to advances in entomologic and vertebrate research, including that on humans.

Introduction

The silkworm *Bombyx mori* is a lepidopteran insect that has been utilized in studies of physiology, genetics, molecular biology, and pathology. Functional analyses of genes related to hormone synthesis/degradation, pheromone reception, larval marking formation, and virus resistance have been performed using this silkworm (Tan et al., 2005; Ito et al., 2008; Sakurai et al., 2011; Daimon et al., 2015; Kondo et al., 2017), and the findings obtained have contributed to the promotion of insect science. The silkworm has the ability to produce large amounts of silk proteins, which is one of the most prominent characteristics of this species. Silk proteins are mainly composed of the fibrous protein Fibroin and aqueous protein Sericin and are produced in the larval tissue silk gland (SG) (Yukuhiro et al., 2016). A transgenic technique has been applied to the silkworm (Tamura et al., 2000), and has enabled the production of a large amount of recombinant proteins through the introduction of transgenes, which are overexpressed in the SG (Tatematsu et al., 2010). Through this method, it is possible to utilize the silkworm as a significant bioreactor.

Based on its biological and industrial importance, the whole genome sequence data of the silkworm was reported in 2004 from two research groups (Mita el al., 2004; Xia et al., 2004), and was the first lepidopteran whole genome data. Silkworm whole genome data was updated in 2008 from an international research group (International Silkworm Genome Consortium 2008). Several data related to the silkworm genome

68 have since become available (e.g. microarray-based gene expression profiles in
69 multiple tissues, BAC-based linkage map full-length cDNA data and of *B. mori* in
70 KaikoBase) (Xia et al., 2007; Yamamoto et al., 2008; Suetsugu et al., 2013). These
71 findings have strongly promoted studies on *B. mori* and other lepidopteran insects in
72 the past decade.
73 In 2019, we reported a new and high-quality genome silkworm reference
74 genome assembly the silkworm p50T strain using PacBio long-read and Illumina short-
75 read sequencers (Kawamoto et al., 2019). The new genome assembly consists of 696
76 scaffolds with N50 of 16.8 M and only 30 gaps, and a new gene model based on this
77 sequence was predicted. These data are expected to be utilized in silkworm and
78 Lepidopteran research. Reference transcriptome data using this genome sequence
79 and the predicted gene set and transcriptome profile of important tissues significantly
80 contribute to advances in silkworm and Lepidopteran research. In the present study,
81 we constructed a reference transcript sequence data set using the RNA-seq data of 10
82 important tissues from silkworm larvae and reference genome data for improving the
83 predicted gene set data of Kawamoto et al. (2019) (Fig. 1). We also showed
84 comprehensive expression data for 10 different organs. These results will contribute
85 to further advances in silkworm as well as entomological and vertebrate research,
86 including that on humans.

87 Results

88 Reference transcriptome data

89 Total RNAs were extracted from the fat body (FB), midgut (MG), Malpighian
90 tubules (MT), testis (TT), anterior silk gland (ASG), anterior part of the middle silk gland
91 (MSG-A), middle part of the middle silk gland (MSG-M), posterior part of the middle silk
92 gland (MSG-P) and posterior silk gland (PSG) of one male P50T larva and from the
93 ovary (OV) of a female larva. Extraction was repeated three times. Total RNAs were
94 sequenced and thirty sets of sequenced data were used as RNA-seq data. We
95 obtained “reference transcriptome data” by using the reference genome, gene model
96 data (Kawamoto et al., 2019), and RNA-seq data. Transcriptome data contains 51,926
97 transcripts in 24236 loci. The previously constructed gene model data contained
98 16,880 genes in 16,845 loci, while our reference transcriptome data contains new
99 transcripts and loci (Fig. 2A). Among 51,926 transcripts, 7,704 belonged to new loci
100 (Fig. 2B); in the gtf file (Supporting data 1), ref_gene_id starts with “MSTRG", which
101 indicated loci or transcripts identified during the construction of the reference
102 transcriptome data, and transcript_id starts with “MSTRG”. A total of 27,342 transcripts

103 is newly identified isoforms (Fig. 2B); ref_gene_id starts with “KWMTBOMO", which
104 indicated that the gene had already been identified in the “gene model data”
105 (Kawamoto et al., 2019), and transcript_id starts with “MSTRG”. These results suggest
106 that our reference transcriptome data extend gene model data and contain many
107 unidentified transcripts and loci. To annotate transcripts, we predicted the coding
108 sequence region (CDS) and amino acid sequences (Supporting data 2) against all
109 transcripts. We found that 39,619 transcripts and 16,632 loci had at least one CDS.
110 The predicted amino acid sequences were used for gene functional annotations by a
111 homology search against human and *Drosophila* gene sets (Supporting data 3).
112
113 Estimating the abundance of the reference transcriptome in multiple tissues
114 We calculated the abundance of each transcript in ten tissues: FB, MG, MT, TT,
115 OV, ASG, MSG-A, MSG-M, MSG-P, PSG, TT, and OV. In comparisons of our
116 calculated results and evaluations of the reliability of our expression analysis, we
117 additionally quantified transcript expression by using public RNA-seq data that were
118 sequenced from the FB, MG, MT, TT, and SG of the *B. mori* o751 strain (Kikuchi et al.,
119 2017; Ichino et al., 2018; Kobayashi et al., 2019). To distinguish between our RNA-seq
120 data and public data, we referred to the FB, MG, MT, TT, and SG of the o751 strain as
121 BN_FB, BM_MG, BN_ MT, BM_TT, and BM_SG, respectively. Abundance values are
122 shown as transcripts per million (tpm) and listed in Supporting data 4.
123 Hierarchical clustering was performed for comparisons of transcriptome
124 abundance between multiple tissues (Fig. 3). The results obtained showed that, except
125 for MSG_P and MSG_M, all samples were clearly grouped by tissue types. Moreover,
126 clusters of samples that were the same tissues, but extracted from different strain
127 larvae, namely, FB and BN_FB, MT and BN_MT, MG and BN_MG, and TT and
128 BN_TT, were placed in adjacent positions, of which samples were obtained from
129 different studies as well as different strains. These results suggest that the data
130 obtained on abundance were highly reproducible and there were a little difference in
131 transcriptome profiles between P50T and o751 larvae. These results also indicated
132 that there were slight individual genetic differences between the larval samples used
133 and a marginal artificial effect, demonstrating that our abundance data may be used as
134 reference expression data for silkworm larvae.
135 Transcripts of *sericin*, *fibroin*, and *fibrohexamerin* genes
136 The *sericin*, *fibroin*, and *fibrohexamerin* (*fhx*) genes are known to play
137 important roles in silk synthesis in *B. mori*. Our transcriptome data contains several
138 isoforms of *sericin*, *fibroin*, *and fhx* (Table 1). A detailed sequence analysis was

139 performed to elucidate isoform structures. A previous analysis of *sericin-1* revealed that
140 this gene is composed of 9 exons, with exons 3-6 being under the selection of
141 alternative splicing (Garel et al., 1997; Yukuhiro et al., 2016). Within these exons, exon
142 6 is responsible for the most abundant component of the sericin protein (Sericin M),
143 which is ~6500 bp in length and encodes a serine-rich repetitive sequence (Yukuhiro et
144 al., 2016). However, the structure of this exon has not yet been elucidated in detail. We
145 herein found that exon 6 of MSTRG.2477.1, the longest *sericin-1* isoform identified in
146 the present study, had a length of 6234 bp (from 2,552,212 to 2,558,445 bp in
147 chromosome 11, see Supporting data 2 and Fig. 4A) In the present study, we newly
148 identified a *sericin-1* isoform that contained exon 6 with 6234 bp. We speculate that
149 this isoform corresponds to the full-length or nearly full-length transcript of *sericin-1*.
150 The product from this exon is enriched with serine residues and also has abundant
151 residues of glycine, asparagine and threonine (Supplemental Fig. 1).
152 Sericin-3 is another major silk protein that has a relatively soft texture (Takasu
153 et al., 2006; 2007). In gene model data, there is a frame shift in the predicted amino
154 acid sequence (KWMTBOMO08464), presumably due to the 73-bp deletion present in
155 exon 3. In the present study, we found that reference transcriptome data
156 (MSTRG.2595.1) provided an accurate gene structure. Sericin-4 is another recently
157 identified sericin protein that is composed of 34 exons (Dong et al., 2019). In gene
158 model data, it is split into three genes (KWMTBOMO06324, KWMTBOMO06325 and
159 KWMTBOMO06326) whereas our reference transcriptome data represent an exact
160 structure (MSTRG.2610.1, Fig. 4B).
161 In contrast, a better structure is provided by gene model data for the fibroin
162 heavy chain (*h-fib*); this gene encodes a protein with a large and highly repetitive
163 sequence (Zhou et al., 2000) and although there is a small deletion in the repeat motifs
164 for both models, the deletion length is shorter for gene model data (32 amino acid
165 deletion for gene model data and 223 for reference transcriptome data). Regarding
166 other silk genes (*sericin-2*, *fibroin light chain* (*l-fib*), and *fhx*), both models provide exact
167 structures (data not shown).
168 Transcript abundance in the silk gland
169 As described above, silk is synthesized in the SG. While the role of each SG
170 part in silk synthesis is known, the underlying molecular and genetic mechanisms
171 remain unclear. Therefore, the genes or transcripts that are strongly expressed in each
172 SG part need to be identified in order to elucidate these mechanisms. We searched for
173 transcripts that showed values of more than 30 transcripts per kilobase million (tpm) in
174 the five SG parts. The results obtained are shown in Fig. 5. The numbers of transcripts

175 that were strongly expressed in only ASG, MSG_A, MSG_M, MSG_P, and PSG were
176 351, 180, 99, 71, and 100, respectively, while more than 1,000 transcripts were
177 strongly expressed in all parts of the SG.
178 By using the annotation data of the strongly expressed transcripts, a functional
179 enrichment analysis (FEA) was performed using the transcripts strongly expressed in
180 each part of the SG to predict their role. In the enrichment analysis, we utilized the
181 annotation results against the human gene set. Fig. 6A shows the results of FEA using
182 the annotation of transcripts strongly expressed in MSG_P, MSG_M specific plus both
183 in MSG_P and MSG_M. The reason for utilizing MSG_P, MSG_M specific plus MSG_P
184 and MSG_M classes is that the samples of MSG_P and MSG_M in Fig. 3 did not form
185 different clusters, suggesting that both tissues have the same functions. The highly
186 enriched function of the category (-log(P) > 10) was “Metabolism of RNA”, while the
187 moderately enriched functions (6 < -log(P) < 10) were “ncRNA metabolic process”,
188 “regulation of mRNA processing”, “HIV Infection”, and “Asparagine N-linked
189 glycosylation”. In MSG_A, the moderately enriched function was “Metabolism of
190 vitamins and cofactors”, while the highly enriched functions of the category were not
191 found (Fig. 6B). In ASG, the highly enriched functions of the category were
192 “carbohydrate metabolic process” and “Transport of small molecules” (Fig. 6C). The
193 moderately enriched functions were “anion transport”, “Glycolysis/Gluconeogenesis”,
194 “Ascorbate and aldarate metabolism”, and “Metabolism of carbohydrates”. In PSG, the
195 moderately enriched function was “tRNA modification”, while the highly enriched
196 function of the category was not found (Fig. 6D).

197 Discussion

198 In the present study, we obtained RNA-seq data on ten tissues of *B. mori* on the
199 3rd day of fifth instar larvae from the P50T strain. Using RNA-seq data and new
200 reference genome data (Kawamoto et al., 2019), we constructed reference
201 transcriptome data. Our transcriptome data contained new loci and isoforms, thereby
202 updating the reference genomic and transcriptome data of *B. mori*. The reference
203 transcriptome consists of 51,926 transcripts in 24,236 loci (16,632 loci have coding
204 genes), and 39,619 transcripts contain single or multiple CDS. In the mouse reference
205 data set (GRCm38.p6), there are 52332 loci (22,480 coding genes, 16,324 non-coding
206 genes, and 13,528 pseudogenes) and 142,333 transcripts
207 (http://asia.ensembl.org/Mus_musculus/Info/Annotation). In the human reference data
208 set (GRCh38.p12), there are 63,048 loci (20,454 coding genes, 23,940 non-coding
209 genes, and 15,204 pseudogenes) and 226,950 transcripts

210 (http://asia.ensembl.org/Homo_sapiens/Info/Annotation). In *Drosophila melanogaster*
211 (BDGP6.22), there are 17,753 loci (13,931 coding genes, 3,513 non-coding genes, and
212 309 pseudogenes) and 34,802 transcripts
213 (http://asia.ensembl.org/Drosophila_melanogaster/Info/Annotation). In Zebrafish
214 (GRCz11), there are 32,506 loci (25,592 coding genes, 6,599 non-coding genes, and
215 315 pseudogenes) and 59,878 transcripts
216 (http://asia.ensembl.org/Danio_rerio/Info/Annotation). In consideration of the basic
217 status of the reference data of these model species, our transcriptome data is not
218 unusual. It suggests that transcriptome data cover the majority of actual transcripts.
219 We estimated transcriptome abundance in multiple tissues plus several
220 tissues of other strain larvae. Transcriptome abundance in the tissues MG, TT, MT,
221 and FB did not markedly differ between the P50T and o751 strains. These results
222 suggest that these tissues at this stage did not contribute to phenotypic differences
223 between the two strains. To elucidate the underlying genetic mechanisms for
224 phenotypic differences, the RNA-seq data and transcriptome data of other stages are
225 needed. On the other hand, transcriptome abundance in MSG_M and MSG_P samples
226 was not divided into two independent clusters, suggesting that both parts have similar
227 roles in this stage, while MSG_A has distinct roles from the other parts.
228 We searched for new or previously unidentified isoforms of the *sericin, fibroin*,
229 *and fhx* genes in reference transcriptome data. While new or previously unidentified
230 isoforms of *sericin-2*, *l-fib*, *h-fib*, and *fhx* were not found, the long or structured isoforms
231 of *Sericin-1, Sericin-3*, and *Sericin-4* were identified in the reference transcriptome. The
232 longest isoform of *Sericin-3* (MSTRG.2595.1) possessed slightly more extensive
233 nucleotide sequences than that of KWMTBOMO08464, in which 73 bases of exon 3
234 were deleted, resulting in the prediction of incorrect ORF. The predicted amino acid
235 sequences of KWMTBOMO08464 were not similar to the sericin-3 amino acid
236 sequence in UniProtKB (ID: A8CEQ1), while that of MSTRG.2595.1 was similar.
237 Therefore, our transcriptome data provide more precise gene predictions. In the case
238 of *Sericin-4*, which was recently identified (Dong et al., 2019), we found a longer
239 transcript in our transcriptome data than the gene model reported by Dong et al.
240 (2019), which may contribute to the further characterization of sericin-4. The new
241 isoform of *Sericin-1* contains CDS that code glycine-, asparagine-, and threonine-rich
242 regions. It was not possible to elucidate the sequences of CDS because they were very
243 repetitive. Using long-read sequencers, repetitive sequences have been accurately
244 elucidated in the new reference genome. We consider our reference transcriptome
245 data to have significantly improved gene model data.

246 We searched for strongly expressed transcripts in one or more SG parts.
247 While more than 1,000 transcripts were strongly and ubiquitously expressed in the SG,
248 801 transcripts were strongly expressed in single parts of the SG. FEA with annotation
249 data on these transcripts in each part of the SG, except for the categories of MSG_A,
250 MSG_M specific plus MSG_A and MSG_M, was performed. The FEA results for
251 MSG_A, MSG_M specific plus MSG_A and MSG_M showed that these parts have
252 roles in coding or non-coding RNA processing. Some functional descriptions of these
253 ontologies are related to "splice variant processing". Some isoforms of *sericin-1* (IDs of
254 MSTRG.2477.1 - MSTRG.2477.16, and KWMTBOMO06216.mrna1) were strongly
255 expressed in MSG_A and MSG_M. Moreover, the FEA result contained "Asparagine
256 N-linked glycosylation". These results suggest that the splice variant processing of
257 *sericin-1* and asparagine processing of the sericin-1 protein, which possesses many
258 asparagine residues, occurred in MSG_A and MSG_M. The FEA results for ASG
259 suggested that ASG produced large amounts of energy via carbohydrate metabolic
260 processes. Silk proteins are mainly synthesized in PSG and MSG. After several
261 processes, matured silk protein, which is a large complex, is exported and released
262 through ASG (Takiya et al., 2016). Therefore, the strong expression of "carbohydrate
263 metabolic"-related transcripts may contribute to the export of silk protein. Since there is
264 moderate ontology for MSG_A and PSG, we cannot predict the roles of these parts.
265 In the present study, we performed RNA-seq on multiple tissues of *B. mori* and
266 constructed reference transcriptome data. The reference transcriptome data
267 constructed using RNA-seq data and new reference genome data contained
268 unidentified loci and isoforms, including a long and almost complete *sericin-1* isoform,
269 which are not present in the gene model data based on a reference new genome
270 (Kawamoto et al., 2019). Moreover, comprehensive transcriptome abundance and
271 annotation data will contribute to elucidating the functions of SG parts previously not
272 proven. The transcript data obtained herein will lead to advances in entomologic and
273 vertebrate research, including that on humans (Tabunoki et al., 2016).

274 Methods

275 <u>Silkworm rearing, RNA extraction, and sequencing</u>

276 The silkworm P50T (*daizo*) strain was reared on an artificial diet (Nihon Nosan
277 Kogyo, Yokohama, Japan) at 25°C under a 12-hour light/dark photoperiod. Tissues of
278 the SG, FB, MG, MT, TT, and OV were dissected on the 3rd day of fifth instar larvae.
279 The SG was further subdivided into ASG, MSG-A, MSG-M, MSG-P, and PSG. Each
280 tissue was dissected from one individual, except for OV, and three biological replicates

281 were obtained and analyzed separately. Tissues were homogenized using ISOGEN
282 (NIPPON GENE, Tokyo, Japan) and the SV Total RNA Isolation System (Promega,
283 Madison, WI) was used for RNA extraction. Extracted total RNA samples were
284 sequenced by Illumina Novaseq6000 (Macrogen Japan Corp., Kyoto, Japan).

285 Construction of reference transcription data and estimation of the expression of
286 each transcript

287 The raw RNA-seq data of 30 samples were trimmed by Trimmomatic-version
288 0.36 (Bolger et al., 2014). The trimmed RNA-seq data of each tissue were mapping to
289 the new reference genome with the new gene model (Kawamoto et al., 2019) by Hisat2
290 version 2.1.0. Each mapped data were assembled to transcriptome data by stringtie
291 version 1.3.3 (Pertea et al., 2016). The 30 transcriptome data sets were merged to one
292 transcriptome data set referred to as "a reference transcriptome" by the stringtie.
293 gffcompare v0.10.6 was used (https://ccb.jhu.edu/software/stringtie/gffcompare.shtml)
294 for comparisons with the reference transcriptome and gene set of Kawamoto et al.
295 (2019).

296 To estimate the expression of the reference transcriptome in 30 samples, the
297 raw fastq data of each sample and reference transcript data were used with Kallisto
298 ver0.44.0 (Bray et al., 2016). In comparisons of transcriptome data, the raw RNA-seq
299 data of multiple tissues in *B. mori* strain o751 from the Sequence Read Archive (SRA)
300 and reference transcript data were used: the accession numbers of raw RNA-seq data
301 are DRA005094, DRA005878 and DRA005094 (Kikuchi et al., 2017; Ichino et al.,
302 2018; Kobayashi et al., 2019).

303 We used TIBCO Spotfire Desktop (v7.6.0) software with the "Better World"
304 program license (TIBCO, Inc., Palo Alto, CA; http://spotfire.tibco.com/better-world-
305 donation-program/) for the classification of differentially expressed samples in silkworm
306 tissues in hierarchical clustering using Ward's method.

307 Annotation for the reference transcriptome and functional enrichment analysis

308 Transcoder (v5.5.0) was used to identify coding regions within transcript
309 sequences and convert transcript sequences to amino acid sequences
310 (https://transdecoder.github.io/).
311 Transcriptome sequence sets were compared at the amino acid sequence level by the
312 successive execution of the blastp program in the NCBI BLAST software package
313 (v2.9.0+) with default parameters and an E-value cut-off of 1e-10 (Altschul et al.,1997).
314 Regarding the reference database sets to be blasted, human and fruit fly (*D.*
315 *melanogaster*) protein datasets in the Ensembl database (v.97) were used because the
316 sequences of these organisms were functionally well-annotated and amenable to

computational methods, such as a pathway analysis (Tabunoki et al., 2013). The names of top-hit genes in the human and fruit fly datasets were annotated to *B. mori* transcripts utilizing Ensembl Biomart (Kinsella et al., 2011) and Spotfire Desktop software under TIBCO Spotfire's "Better World" program license (TIBCO Software, Inc., Palo Alto, CA, USA) (https://spotfire.tibco.com/better-world-donation-program/). Functional enrichment analyses were performed using the metascape portal site with annotation results against the human gene set (URL: http://metascape.org/gp/index.html#/main/step1, Zhou et al., 2019).

Investigation of gene structures of *sericin*, *fibroin*, and *fhx*

In investigations on the *sericin*, *fibroin*, and *fhx* gene structures, we visualized the positions of the new gene set and reference transcript data in the new reference genome (Kawamoto et al., 2019) using the Integrative genomics viewer (IGV) (James et al., 2011). In the gene model data set, *sericin-1* corresponded to KWMTBOMO06216, *sericin-2* KWMTBOMO06334, *sericin-3* KWMTBOMO06311, *sericin-4* KWMTBOMO06324-06326, fibroin heavy chain (*h-fib*) KWMTBOMO15365, fibroin light chain *l-fib* KWMTBOMO08464, and *fhx* KWMTBOMO01001. The structures of these models were compared visually with our new reference transcriptome data. The several isoforms identified are listed in Table 1. We performed sequence alignment using gene model sequence data and public sequences deposited in the NCBI database.

Data Availability

The RNA-seq reads supporting the conclusions of this study are available in the SRA with accession number DRA008737 (The accession number of RNA-seq data of each sample is shown in Table 2A).
Assembled transcriptome sequences are available at the Transcriptome Shotgun Assembly (TSA) database under accession IDs ICPK01000001-ICPK01051926.
The estimated abundance of transcripts is available from the Gene Expression Archive (GEA) in DDBJ under accession ID E-GEAD-315.
Supporting data are available in The Life Science Database Archive. The title in the Archive is "KAIKO - Metadata of reference transcriptome data" (DOI:10.18908/lsdba.nbdc02443-000.V001).

References

349 Altschul, S.F. et al. "Gapped BLAST and PSI-BLAST: a new generation of protein
350 database search programs." Nucleic Acids Research 25:3389-3402 (1997). DOI:
351 10.1093/nar/25.17.3389
352 Bolger, A. M. et al. Trimmomatic: A flexible trimmer for Illumina Sequence Data.
353 Bioinformatics, btu170 (2014). DOI: 10.1093/bioinformatics/btu170
354 Bray, N. L. et al. Near-optimal probabilistic RNA-seq quantification. Nature
355 Biotechnology 34:525–527 (2016). DOI: 10.1038/nbt.3519
356 Daimon, T. et al. Knockout silkworms reveal a dispensable role for juvenile hormones
357 in holometabolous life cycle. Proceedings of the National Academy of Sciences of
358 the United States of America 112 E4226-E4235 (2015). DOI:
359 10.1073/pnas.1506645112
360 Dong, Z. et al. Identification of *Bombyx mori* sericin 4 protein as a new biological
361 adhesive. International Journal of Biological Macromolecules 132:1121-1130 (2019).
362 DOI: 10.1016/j.ijbiomac.2019.03.166
363 Garel, A. et al. Structure and organization of the *Bombyx mori* sericin 1 gene and of the
364 sericins 1 deduced from the sequence of the Ser 1B cDNA. Insect Biochemistry and
365 Molecular Biology 27:469–477 (1997). DOI: 10.1016/S0965-1748(97)00022-2
366 Ichino, F. et al. Construction of a simple evaluation system for the intestinal absorption
367 of an orally administered medicine using *Bombyx mori* larvae. Drug Discoveries and
368 Therapeutics 12:7-15 (2018). DOI: 10.5582/ddt.2018.01004
369 International Silkworm Genome Consortium. The genome of a lepidopteran model
370 insect, the silkworm Bombyx mori. 38(12):1036-45 (2008). DOI:
371 10.1016/j.ibmb.2008.11.004.
372 Ito, K. et al. Deletion of a gene encoding an amino acid transporter in the midgut
373 membrane causes resistance to a *Bombyx* parvo-like virus. Proceedings of the
374 National Academy of Sciences of the United States of America 105 7523-7527
375 (2008). DOI: 10.1073/pnas.0711841105
376 James, T. et al. Integrative genomics viewer. Nature Biotechnology 29:24–26 (2011).
377 DOI: 10.1038/nbt.1754
378 Kawamoto, M. et al. High-quality genome assembly of the silkworm, Bombyx mori.
379 Insect Biochemistry and Molecular Biology 107:53-62 (2019). DOI:
380 10.1016/j.ibmb.2019.02.002
381 Kikuchi, A. et al. Identification of functional enolase genes of the silkworm *Bombyx mori*
382 from public databases with a combination of dry and wet bench processes. BMC
383 Genomics 18: 83 (2017). DOI: 10.1186/s12864-016-3455-y

384 Kinsella, R.J. et al. Ensembl BioMarts: a hub for data retrieval across taxonomic space.
385 Database (Oxford) 2011:bar030 (2011). DOI: 10.1093/database/bar030
386 Kobayashi, Y. et al. Comparative analysis of seven types of superoxide dismutases for
387 their ability to respond to oxidative stress in *Bombyx mori*. Scientific Reports 9, 2170
388 (2019). DOI: 10.1038/s41598-018-38384-8
389 Kondo, Y. et al. Toll ligand Spätzle3 controls melanization in the stripe pattern
390 formation in caterpillars. Proceedings of the National Academy of Sciences of the
391 United States of America 114 8336-8341 (2017). DOI: 10.1073/pnas.1707896114
392 Mita, K. et al. The genome sequence of silkworm, *Bombyx mori.* DNA Research
393 29;11(1):27-35 (2004). DOI:10.1093/dnares/11.1.27
394 Pertea, M. et al. Transcript-level expression analysis of RNA-seq experiments with
395 HISAT, StringTie and Ballgown. Nature Protocols 11:1650-1667 (2016).
396 DOI:10.1038/nprot.2016.095
397 Sakurai, T. et al. A single sex pheromone receptor determines chemical response
398 specificity of sexual behavior in the silkmoth *Bombyx mori*. PLoS Genetics
399 7:e1002115 (2011). DOI 10.1371/journal.pgen.1002115
400 Suetsugu, Y. et al. Large scale full-Length cDNA sequencing reveals a unique
401 genomic landscape in a lepidopteran model insect, *Bombyx mori*. G3 3(9):1481-
402 1492 (2013). DOI:10.1534/g3.113.006239
403 Takiya, S. et al. Regulation of Silk Genes by Hox and Homeodomain Proteins in the
404 Terminal Differentiated Silk Gland of the Silkworm *Bombyx mori*. Journal of
405 Developmental Biology 4(2):19 (2016). DOI:10.3390/jdb4020019
406 Tabunoki, H. et al. Can the silkworm (Bombyx mori) be used as a human disease
407 model? Drug Discoveries and Therapeutics 10:3-8 (2016).
408 DOI:10.5582/ddt.2016.01011
409 Takasu, Y. et al. The silk sericin component with low crystallinity. Sanshi-Konchu
410 Biotec 75:133–139 (2006) DOI: 10.11416/konchubiotec.75.133
411 Takasu, Y. et al. Identification and characterization of a novel sericin gene expressed
412 in the anterior middle silk gland of the silkworm *Bombyx mori*. Insect Biochemistry
413 and Molecular Biology 37:1234–1240 (2007) DOI: 10.1016/j.ibmb.2007.07.009
414 Tamura, T. et al. Germline transformation of the silkworm *Bombyx mori* L. using a
415 piggyBac transposon-derived vector. Nature Biotechnology 18:81–84 (2000)
416 DOI:10.1038/71978
417 Tan, A. et al. Precocious metamorphosis in transgenic silkworms overexpressing
418 juvenile hormone esterase. Proceedings of the National Academy of Sciences of the

United States of America. 102:11751-11756. (2005) DOI: 10.1073/pnas.0500954102

Tatematsu, K. et al. Construction of a binary transgenic gene expression system for recombinant protein production in the middle silk gland of the silkworm *Bombyx mori*. Transgenic Research, 19:473-487 (2010). DOI:10.1038/71978

Xia, Q. et al. A draft sequence for the genome of the domesticated silkworm (*Bombyx mori*). Science 10;306(5703):1937-40 (2004). DOI:10.1126/science.1102210

Xia, Q. et al. Microarray-based gene expression profiles in multiple tissues of the domesticated silkworm, *Bombyx mori*. Genome Biology 8(8):R162 (2007). DOI:10.1186/gb-2007-8-8-r162

Yamatomo, K. et al. A BAC-based integrated linkage map of the silkworm Bombyx mori. Genome Biology. 9:R21 (2008). DOI:10.1186/gb-2008-9-1-r21

Yukuhiro, K. et al. Insect silks and cocoons: structural and molecular aspects. Extracellular composite matrices in Arthropods (eds. E. Cohen & B. Moussian), pp.515-555. Springer, Cham. (2016) DOI: 10.1007/978-3-319-40740-1_18

Zhou, C. et al. Fine organization of *Bombyx mori* fibroin heavy chain gene. Nucleic Acids Research 28:2413–2419 (2000). DOI: 10.1093/nar/28.12.2413

Zhou, Y. et al. Metascape provides a biologist-oriented resource for the analysis of systems-level datasets. Nature Communications 10(1):1523 (2019). DOI:10.1038/s41467-019-09234-6

Funding

This work was supported by the National Bioscience Database Center of the Japan Science and Technology Agency (JST) to HB.

This work was supported by the Cabinet Office, Government of Japan, Cross-ministerial Strategic Innovation Promotion Program (SIP), “Technologies for Smart Bio-industry and Agriculture” (funding agency: Bio-oriented Technology Research Advancement Institution, NARO) to KY, TT, JS, and HS.

This work was supported by a grant from the Ministry of Agriculture, Forestry and Fisheries of Japan (Research Project for Sericultural Revolution) to KY, TT, and HS.

Acknowledgments

The computing resource was partly provided by the super computer system at the National Institute of Genetics (NIG), Research Organization of Information and Systems (ROIS), Japan.

453 # Author contributions

454 Conceived and designed the experiments: K.Y., T.T., and H.S.
455 Performed the experiments: T.T.
456 Contributed reagents/materials/analysis tools: H.S.
457 Analyzed the data: K.Y., J.S., A.J., and H.B.
458 Contributed to the writing of the manuscript under draft version: K.Y., T.T., and H.B.
459 All authors discussed the data and helped with manuscript preparation. K.Y.
460 supervised the project.
461 All authors read and approved the final manuscript.

462 # Competing interests

463 The authors declare no conflicts of interest.

464 # Figures

465 Fig. 1 Workflow of the data analysis performed in the present study. To obtain
466 reference transcriptome sequences, Fastq data of 10 tissues from 5th instar larvae
467 were mapped to the new reference genome (Kawamoto et al., 2019). Kallisto software
468 was used to estimate the expression abundance of each transcript in these tissues
469 plus other *B. mori* samples of which RNA-seq data were obtained from a public
470 database (Accession numbers are listed in Table 2B). We performed a Blast search
471 against human and *Drosophila* genome data to perform functional annotations of the
472 reference transcriptome. Insect, human, database image, and sequencer drawings
473 (http://togotv.dbcls.jp/ja/pics.html) are licensed at
474 (http://creativecommons.org/licenses/by/4.0/deed.en).

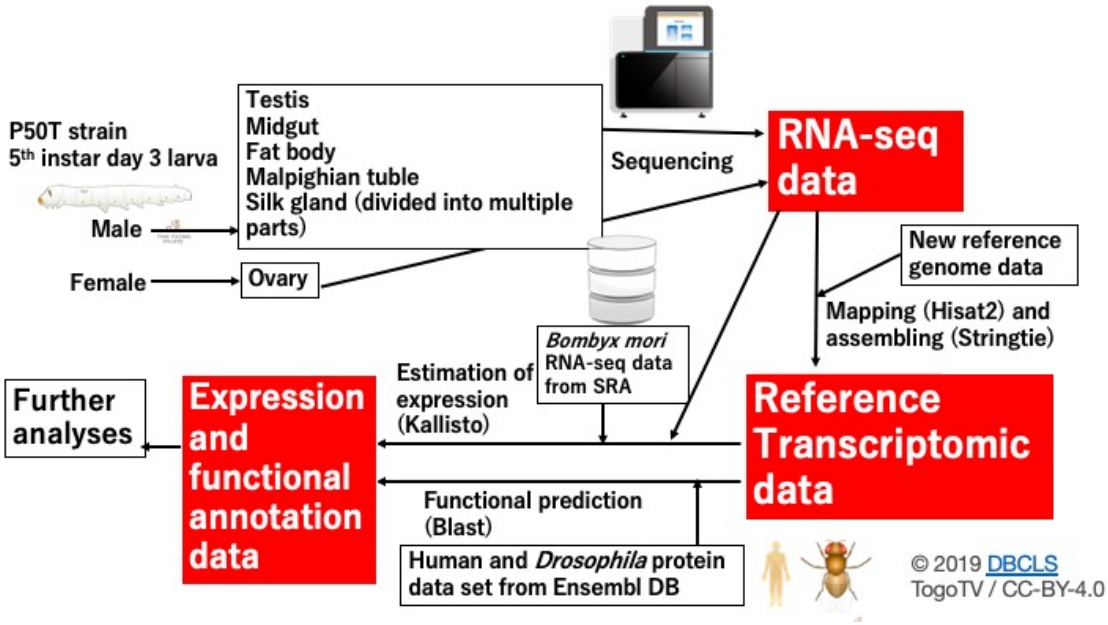

Fig. 2 Basal characteristics of the reference transcriptome. (A) Comparison of gene model data (Kawamoto et al., 2019) and the reference transcriptome data of the present study. The number of loci and transcripts are shown. These numbers were calculated from gff files of the two data sets. (B) Classification of 51,926 transcripts. Each transcript was classified into three categories, and the numbers of the three categories are shown in a pie chart. Definitions of the three categories were described in the main text.

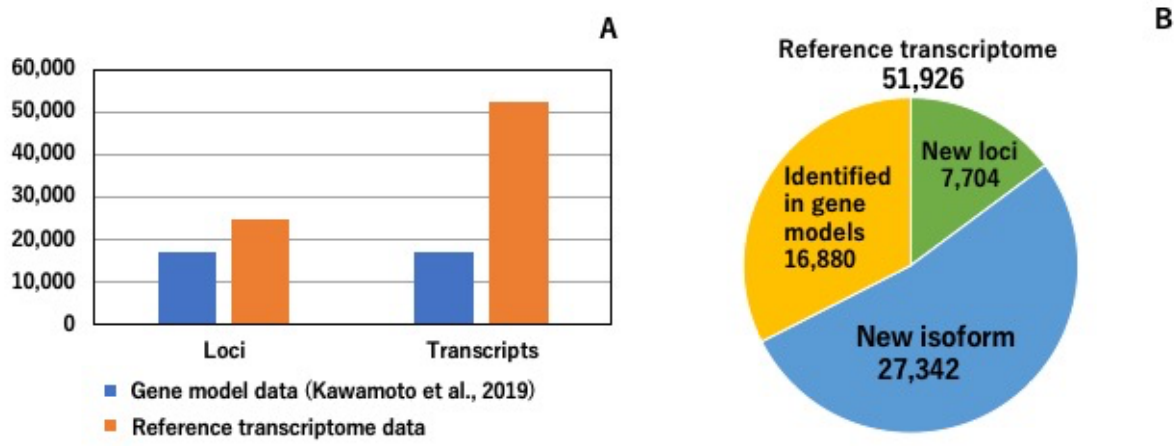

Fig. 3 Hierarchical clustering of expression data in 45 samples. Hierarchical clustering was performed using transcriptome expression data (tpm values). Abbreviations of the samples are shown and described in the main text. The numbers added to the

abbreviations mean biological replicates.

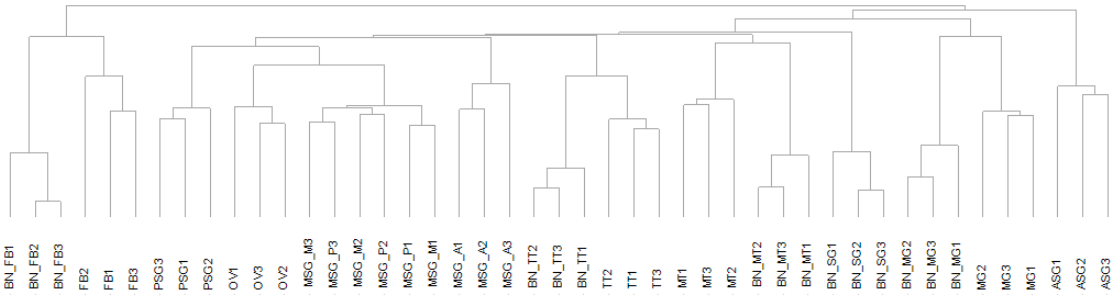

Fig. 4 Longest isoforms of *sericin-1* and *sericin-4* in the reference transcriptome. (A) A schematic drawing showing the exon positions of isoform MTSRG.2477.1 (longest isoform of *sericin-1*) and a gene model of *sericin-1* (Kawamoto et al., 2019). Squares indicate exons with exon numbers in the gff file (Supporting data 1). Exon 6 of MSTRG.2477.1 corresponds to exon 5' and exons 7-10 correspond to exons 6-9 in KWMTBOMO06216 (each group of exons are connected with dashed lines).

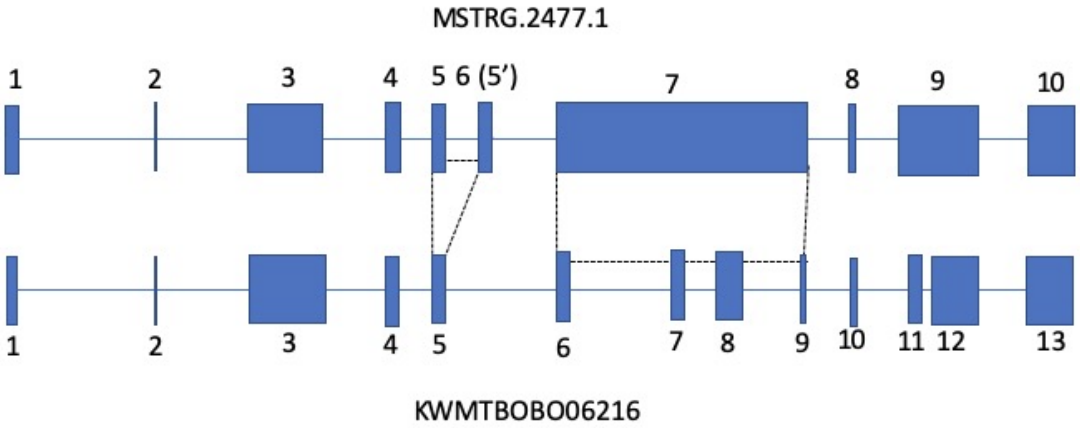

(B) Exon positions of isoform MTSRG.2477.1 (the longest isoform of *sericin-4*) and the gene model of *sericin-4* (KWMTBOMO06325, KWMTBOMO06325, and KWMTBOMO06326) in the new reference genome is shown by IGV. The scale above the transcript indicates the location of chromosome 11.

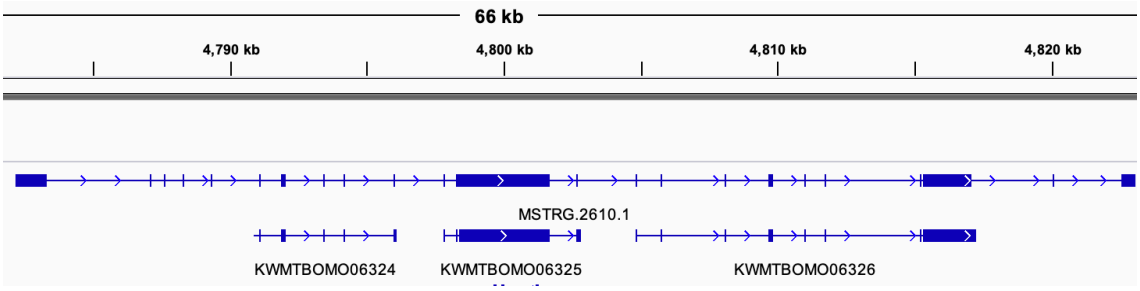

Fig. 5 Strongly expressed transcripts within the silk gland. The numbers in the Venn diagrams indicate the number of transcripts of which values of tpm were more than 30 in the corresponding silk gland parts.

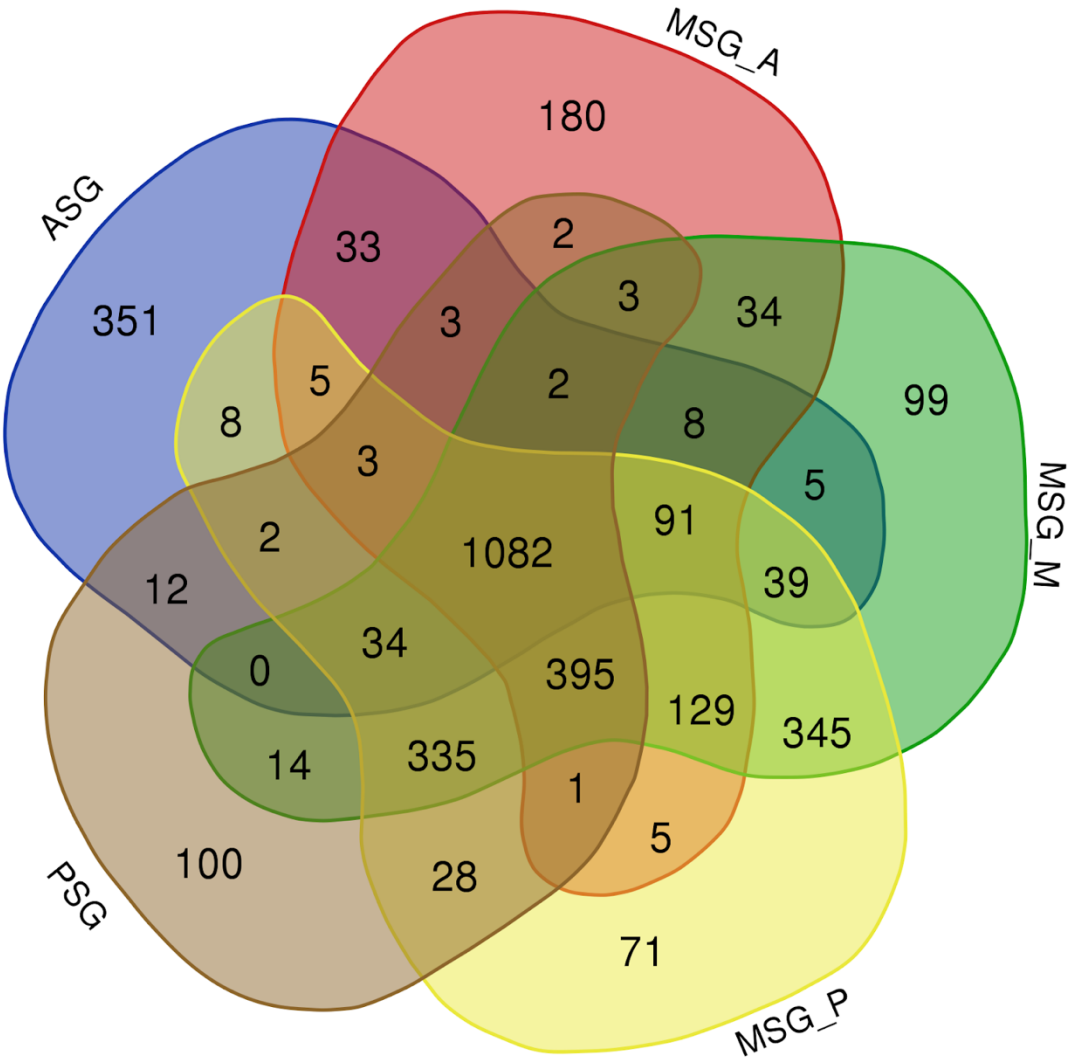

Fig. 6 Results of the enrichment analysis by Metascape. Using annotation data against the human gene set of the reference transcripts expressed in one or several parts of the silk gland (Fig. 5), an enrichment analysis was performed (numbers in brackets after the silk gland parts indicate the numbers of transcripts). -log10 (P) represents -log10 (P-value). For example, -log10 (P)=5 represents P-value= 10^{-5} (A) Transcripts showing tpm > 30 in MGM_M (99),MGM_P (71), and MGM_M and MGM_P (345).

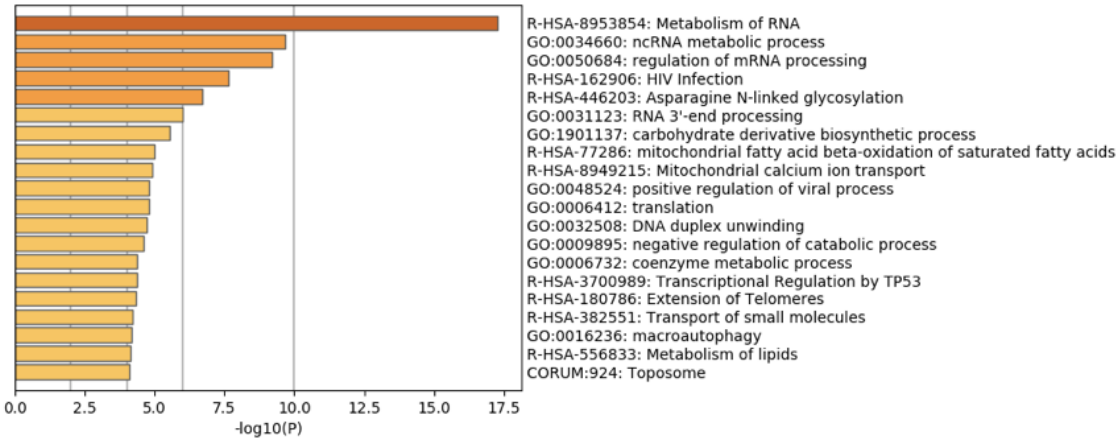

(B) Transcripts showing tpm > 30 in MSG_A (180).

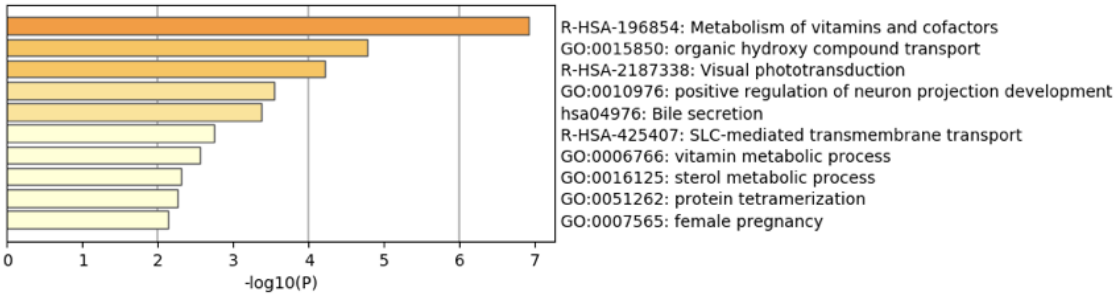

(C) Transcripts showing tpm > 30 in ASG (351).

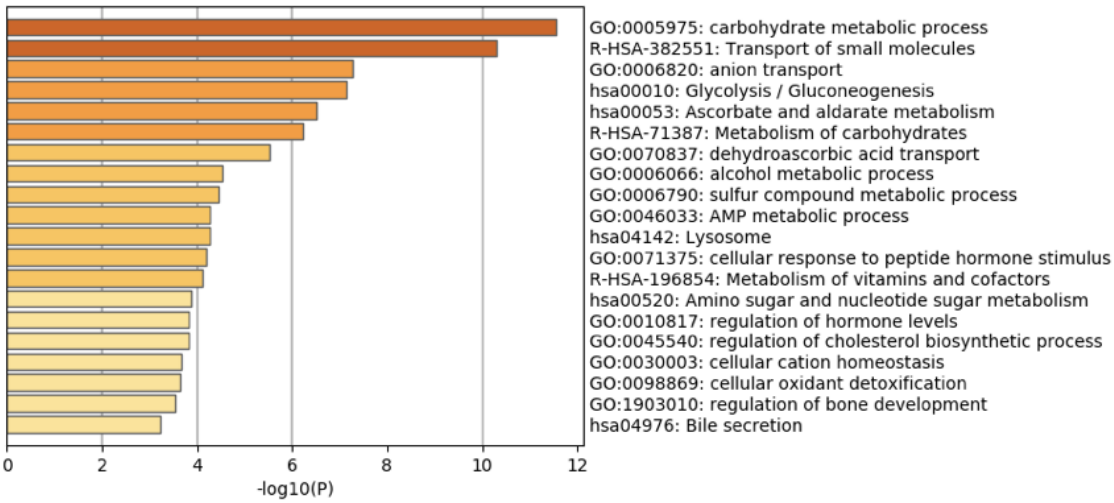

(D) Transcripts showing tpm > 30 in PSG (100).

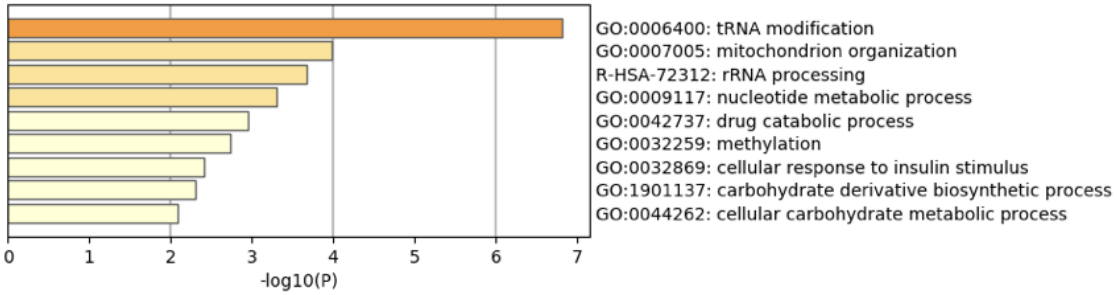

Table

Table 1

Sericin, fibroin, and *fibrohexamerin* genes and isoform IDs

Gene name	Gene model ID in Kawamoto et al., 2019	Isoform IDs in Supporting data 1 (GenBank IDs)
sericin-1	KWMTBOMO06216	MSTRG.2477.1 - MSTRG.2477.16, KWMTBOMO06216.mrna1 (ICPK01006046 -ICPK01006062)
sericin-2	KWMTBOMO06334	MSTRG.2627.1, MSTRG.2627.2, KWMTBOMO06334.mrna1 (ICPK01006484 -ICPK01006486)
sericin-3	KWMTBOMO06311	MSTRG.2595.1 - MSTRG.2595.9, KWMTBOMO06311.mrna1 (ICPK01006421 -ICPK01006430)
sericin-4	KWMTBOMO06324-06326	MSTRG.2610.1 (ICPK01006453)
fibroin heavy chain (*h-fib*)	KWMTBOMO15365	MSTRG.14927.1 - MSTRG.14927.23, KWMTBOMO15365.mrna1 (ICPK01035046 -ICPK01035068)

fibroin light chain (*l-fib*)	KWMTBOMO08464	MSTRG.5511.1, KWMTBOMO08464.mrna1 (ICPK01013031 -ICPK01013032)
fibrohexamerin	KWMTBOMO01001	

523

524 Table 2

525 A. Samples for RNA-seq and run accession IDs

Sample	SRA Run ID	Sex
Anterior silk gland (ASG)	DRR186474, DRR186475, DRR186476	Male
Anterior part of the middle silk gland (MSG_A)	DRR186477, DRR186478, DRR186479	Male
Middle part of the middle silk gland (MSG_M)	DRR186480, DRR186481, DRR186482	Male
Posterior part of the middle silk gland (MSG_P)	DRR186483, DRR186484, DRR186485	Male
Posterior silk gland (PSG)	DRR186486, DRR186487, DRR186488	Male
Fat body (FB)	DRR186489, DRR186490, DRR186491	Male
Midgut (MG)	DRR186492, DRR186493, DRR186494	Male
Malpighian tubules (MT)	DRR186495, DRR186496, DRR186497	Male
Testis (TT)	DRR186498, DRR186499, DRR186500	Male

Ovary (OV)	DRR186501, DRR186502, DRR186503	Female

B. RNA-seq data from SRA

Sample	SRA Run ID	Reference
Testis	DRR068893, DRR068894, DRR068895	Kikuchi et al. 2017
Fat body	DRR095105, DRR095106, DRR095107	Kobayashi et al. 2019
Midgut	DRR095108, DRR095109, DRR095110	Ichino et al. 2018
Malpighian tubules	DRR095111, DRR095112, DRR095113	Kobayashi et al. 2019
Silk gland	DRR095114, DRR095115, DRR095116	Kobayashi et al. 2019

Supporting data

All supporting data are available in The Life Science Database Archive (https://dbarchive.biosciencedbc.jp/index-e.html).

Supporting data 1
Metadata of reference transcriptome data
URL:https://togodb.biosciencedbc.jp/db/kaiko_trascnript_data
DOI:10.18908/lsdba.nbdc02443-001.V001

Supporting data 2
Predicted amino acid sequences of the reference transcriptome
DOI:10.18908/lsdba.nbdc02443-004.V001

Supporting data 3
Annotations of each transcript (blast against human and *Drosophila* gene sets)

URL:https://togodb.biosciencedbc.jp/db/kaiko_annotation_human_drosophila_data
DOI:10.18908/lsdba.nbdc02443-003.V001

Supporting data 4
Expression data of each transcript in multiple tissues
URL:https://togodb.biosciencedbc.jp/db/kaiko_transcript_tpm_data
DOI:10.18908/lsdba.nbdc02443-002.V001

Supplemental Figure

Supplemental Fig. 1
Predicted amino acid sequences of the longest *sericin1* isoforms (MSTRG.2477.1.p1). Glycine, asparagine and threonine residues are colored in red. The region of exon7 is underlined.
DOI:10.6084/m9.figshare.998056